

Color excesses of type Ia supernovae from the single-degenerate channel model *

Xiang-Cun Meng¹, Xue-Fei Chen², Zhan-Wen Han² and Wu-Ming Yang¹

¹ School of Physics and Chemistry, Henan Polytechnic University, Jiaozuo 454000, China;
xiangcunmeng@hotmail.com

² National Astronomical Observatories/Yunnan Observatory, Chinese Academy of Sciences, Kunming 650011, China

Received 2009 May 21; accepted 2009 July 15

Abstract The single degenerate model is the most widely accepted progenitor model of type Ia supernovae (SNe Ia), in which a carbon-oxygen white dwarf (CO WD) accretes hydrogen-rich material from a main sequence or a slightly evolved star (WD+MS) to increase its mass, and explodes when its mass approaches the Chandrasekhar mass limit. During the mass transfer phase between the two components, an optically thick wind may occur and the material lost as wind may exist as circumstellar material (CSM). Searching for the CSM around a progenitor star is helpful for discriminating different progenitor models of SNe Ia. In addition, the CSM is a source of color excess. The purpose of this paper is to study the color excess produced from the single-degenerate progenitor model with an optically thick wind, and reproduce the distribution of color excesses of SNe Ia. Meng et al. systemically carried out binary evolution calculations of the WD+MS systems for various metallicities and showed the parameters of the systems before Roche lobe overflow and at the moment of supernova explosion in Meng & Yang. With the results of Meng et al., we calculate the color excesses of SNe Ia at maximum light via a simple analytic method. We reproduce the distribution of color excesses of SNe Ia by our binary population synthesis approach if the velocity of the optically thick wind is taken to be an order of magnitude of 10 km s^{-1} . However, if the wind velocity is larger than 100 km s^{-1} , the reproduction is bad.

Key words: stars: white dwarfs — stars: supernova: general

1 INTRODUCTION

Although type Ia supernovae (SNe Ia) have shown their importance in determining cosmological parameters, e.g. Ω_M and Ω_Λ (Riess et al. 1998; Perlmutter et al. 1999), the progenitor systems of SNe Ia have not yet been confidently identified (Hillebrandt & Niemeyer 2000; Leibundgut 2000). It is widely believed that an SN Ia is from the thermonuclear runaway of a carbon-oxygen white dwarf (CO WD) in a binary system. The CO WD accretes material from its companion to increase its mass. When its mass reaches its maximum stable mass, it explodes as a thermonuclear runaway and almost half of the WD mass is converted into radioactive nickel-56 (Branch 2004). Two basic scenarios have been discussed over the last three decades. One is a single degenerate (SD) model, which is widely accepted (Whelan & Iben 1973). In this model, a CO WD increases its mass by accreting hydrogen- or helium-rich matter

* Supported by the National Natural Science Foundation of China.

from its companion, and explodes when its mass approaches the Chandrasekhar mass limit. The companion may be a main-sequence star (WD+MS) or a red-giant star (WD+RG) (Yungelson et al. 1995; Li & van den Heuvel 1997; Hachisu et al. 1999a, Hachisu et al. 1999b; Nomoto et al. 1999, 2003; Langer et al. 2000; Han & Podsiadlowski 2004; Chen & Li 2007; Han 2008; Meng et al. 2009; Lü et al. 2009). An alternative is the theoretically less favored double degenerate (DD) model (Iben & Tutukov 1984; Webbink 1984), in which a system consisting of two CO WDs loses orbital angular momentum by gravitational wave radiation and finally merges. The merger may explode if the total mass of the system exceeds the Chandrasekhar mass limit (see the reviews by Hillebrandt & Niemeyer 2000 and Leibundgut 2000). In theory, a large amount of circumstellar material (CSM) may be produced via an optically thick wind for the SD model (Hachisu et al. 1996), while there is no CSM around DD systems. Thus, a basic method to distinguish the two progenitor models is to find the CSM around progenitor systems.

Evidence for CSM was first found in SN 2002ic (Hamuy et al. 2003), which has shown extremely pronounced hydrogen emission lines that have been interpreted as a sign of strong interaction between supernova ejecta and CSM. The discovery of SN 2002ic may uphold the SD model (Han & Podsiadlowski 2006). Recently, evidence for CSM was found in a normal SN Ia (SN 2006X) defined by Branch, Fisher & Nugent (1993) and the CSM is proposed to be from the wind from a red-giant companion (Patat et al. 2007a). The CSM may play a key role in solving the problem of the low value of the reddening ratio of an external galaxy (Wang 2005), which is very important for precision cosmology (Wang et al. 2008).

If an SN Ia is surrounded by a large amount of CSM, its observed color should be redder than its intrinsic color, which results in a color excess, $E(B - V)$. Reindl et al. (2005) showed the color excesses of more than one hundred SNe Ia at maximum light, which suggests a mission to check which progenitor model of SNe Ia can explain the distribution of the color excesses. Recently, Meng et al. (2009) performed binary stellar evolution calculations for more than 25 000 close WD binary systems with various metallicities, and presented all the parameters of the systems for SNe Ia before Roche lobe overflow (RLOF) and at the moment of supernova explosion in a subsequent paper (Meng & Yang 2009). In their works, the prescription of Hachisu et al. (1999a) for the accretion efficiency of hydrogen-rich material was adopted by assuming an optically thick wind (Hachisu et al. 1996), and then their works provide a possibility to check whether or not the SD model with an optically thick wind can reproduce the distribution of color excesses of SNe Ia obtained from observation. The purpose of this paper is to check this possibility, and this work is based on the results from Meng et al. (2009).

In Section 2, we describe our model. We show the results in Section 3 and give discussions and conclusions in Sections 4 and 5.

2 MODEL AND PHYSICS INPUTS

2.1 Mass Distribution of Lost Hydrogen-rich Material

As described in Section 1, the color of a supernova is reddened by the CSM surrounding the supernova. We first check whether there exists enough CSM resulting from an optically thick wind. The following is a simple description about how to obtain the CSM. As described in Meng et al. (2009), in a WD + MS system, the companion fills its Roche lobe at MS or during HG, and transfers material onto the WD. If the mass-transfer rate, $|\dot{M}_2|$, exceeds a critical value, \dot{M}_{cr} , we assume that the accreted hydrogen steadily burns on the surface of the WD and that the hydrogen-rich material is converted into helium at the rate of \dot{M}_{cr} . The unprocessed matter is assumed to be lost from the system as an optically thick wind at a rate of $\dot{M}_{\text{wind}} = |\dot{M}_2| - \dot{M}_{\text{cr}}$ (Hachisu et al. 1996). Adopting the prescription of Hachisu et al. (1999a) on WDs accreting hydrogen-rich material from their companions, Meng et al. (2009) obtained the initial parameters of WD+MS systems for SNe Ia, and at the same time, the final parameters at the moment of the SN Ia explosion, such as M_2^{SN} . In this paper, incorporating the binary evolution results in Meng et al. (2009) into the rapid binary evolution code developed by Hurley et al. (2000, 2002), we carry out a series of binary population synthesis (BPS) studies for various Z . In each BPS

study, 10^7 binaries are generated by Monte Carlo simulation and a circular orbit is assumed for all binaries. The basic parameters for the simulations are the same as those in Meng et al. (2009). It can be shown that a WD+MS system may originate from three possible evolution channels, namely, the He star channel, the EAGB channel and the TPAGB channel (see Meng et al. 2009 for details). We assume that an SN Ia is produced if the initial parameters of a WD+MS system, e.g. initial orbital period P_{orb}^i and initial secondary mass M_2^i , are located in the appropriate regions of the parameters for SNe Ia at the onset of RLOF. We can obtain the companion mass at the moment of explosion by interpolation in the three-dimensional grid $(M_{\text{WD}}^i, M_2^i, \log P^i)$ of the more than 25000 close WD binary systems calculated in Meng et al. (2009). In Figure 1, we show the mass distribution of hydrogen-rich material lost as the optically thick wind for various metallicities, $M_{\text{wind}} = (M_2^i + M_{\text{WD}}^i) - (M_2^{\text{SN}} + M_{\text{WD}}^{\text{SN}})$, where superscripts i and SN represent the initial and final values for the white dwarf and secondary, respectively, and $M_{\text{WD}}^{\text{SN}}$ is assumed to be $1.378 M_{\odot}$. We can see from the figure that the distribution of the lost mass peaks at about $0.3 M_{\odot}$ and has a high-mass tail. The amount of material lost may be as large as $2.5 M_{\odot}$, which should contribute to the color excess of SNe Ia.

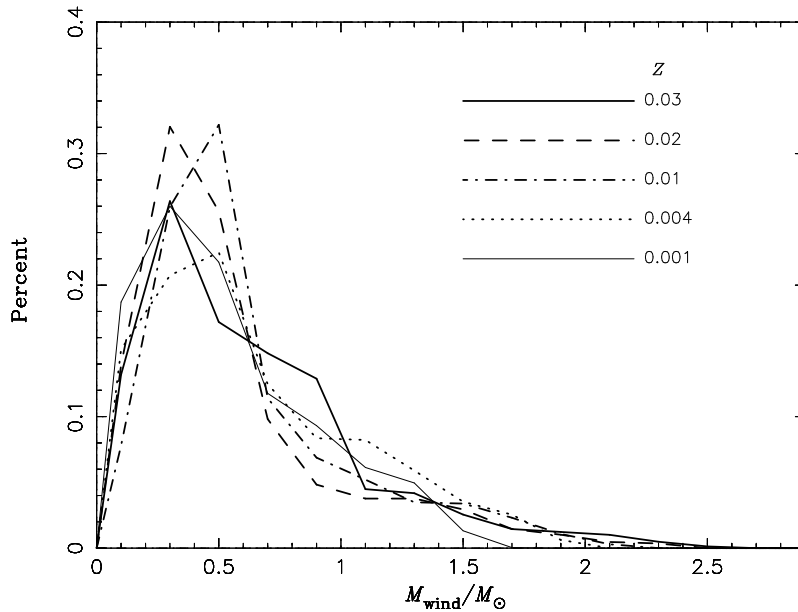


Fig. 1 Mass distribution of hydrogen-rich material lost as optically thick wind for different metallicities.

In Figure 1, we can see that there does not seem to be a systemic trend with metallicity. Actually, the influence of metallicity on the M_{wind} is complicated. M_{wind} is mainly determined by M_2^i and M_{WD}^i . The two parameters are both systemically affected by metallicity, but the tendency is reversed, i.e. the peak of the distribution of the companion moves to higher mass with metallicity, while the peak for WD mass moves to lower mass (see figs. 9 and 10 in Meng et al. 2009). In addition, the metallicity also affects the mass-transfer rate between the WD and its companion, and then M_2^{SN} (Langer et al. 2000). The complicated influence of metallicity on the distribution of M_{wind} results in a non-systemic trend of the distribution with metallicity. We also noticed that the percentage of high M_{wind} , e.g. $M_{\text{wind}} > 2.0 M_{\odot}$, increases with metallicity. High M_{wind} is mainly determined by the upper boundary of the companion mass, which moves to higher mass with metallicity (see fig. 4 in Meng et al. 2009). So, a binary system which produces an SN Ia with high metallicity may lose more hydrogen-rich material by optically thick wind, and then the high-metallicity model in Figure 1 shows a higher percentage of high M_{wind} .

2.2 Model

Bohlin et al. (1978) found

$$E(B - V)/n_{\text{H}} = 1.72 \times 10^{-22} \text{ mag cm}^2, \quad (1)$$

for the Galaxy, where n_{H} is the total hydrogen column density and this relation linearly depends on metallicity (Draine 2003). The linear relation can be fitted by

$$E(B - V)/n_{\text{H}} = (17.4 \times Z/Z_{\odot} - 0.454) \times 10^{-23} \text{ mag cm}^2, \quad (2)$$

where the fitting data are from Bohlin et al. (1978), Koorneef (1982), Fitzpatrick (1985) and Martin et al. (1989). In the following, we describe how to obtain the total hydrogen column density, n_{H} .

While the CSM around the progenitor of an SN Ia may be asymmetric, for simplicity, we assume that the mass loss of the optically thick wind is spherically symmetric and the mass-loss rate is constant during the whole mass-transfer phase. Then, hydrogen number density is only a function of the distance of wind material from the progenitor star, i.e.

$$n(r) = ar^{-2}, \quad (3)$$

where a is a coefficient determined by

$$\int_{r_0}^{r_m} ar^{-2} \cdot 4\pi r^2 dr = N_{\text{H}}, \quad (4)$$

where r_0 is the radius of the progenitor, r_m is the maximum distance to which hydrogen-rich material can arrive as an optically thick wind at the moment of an SN Ia explosion, and N_{H} is the total number of hydrogen atoms. The total hydrogen column density at maximum light is calculated from

$$\int_{r_1}^{r_m} ar^{-2} dr = n_{\text{H}}, \quad (5)$$

where r_1 is the distance of the explosion ejecta from the explosion center at maximum light. From Equations (4) and (5), we can obtain

$$n_{\text{H}} = \frac{N_{\text{H}}}{4\pi r_m r_1}. \quad (6)$$

N_{H} can be obtained from

$$N_{\text{H}} = \frac{XM_{\text{wind}}}{m_{\text{H}}}, \quad (7)$$

where M_{wind} is the total mass lost as optically thick wind, m_{H} is the mass of a hydrogen atom and X is the mass fraction of hydrogen and is set to be

$$X = 0.76 - 3.0Z, \quad (8)$$

(Pols et al. 1998). We can obtain r_m from

$$r_m = V_{\text{wind}} t_d, \quad (9)$$

where V_{wind} is the velocity of the optically thick wind, and t_d is the delay time from the onset of mass transfer to the moment of the SN Ia explosion. From the results of Meng et al. (2009), t_d can be approximated by

$$\log(t_d/\text{yr}) = -\frac{2}{3}M_2^i + 7.8, \quad (10)$$

where M_2^i is the initial mass of the secondary (the mass donor unit in solar mass) in a WD+MS system. From the equation t_d is a rough estimation of the mean value for a certain M_2^i and has an error of about

50%. In addition, r_1 , the distance of the explosion ejecta from the explosion center at maximum light, can be obtained by the product of the velocity of supernova ejecta and the rise time of the light curve of SNe Ia. We simply assume that the velocity of ejecta is $10\,000\text{ km s}^{-1}$ (Gamezo et al. 2003) and the rise time of the light curve of SNe Ia is 20 d (Conley et al. 2006; Strovink 2007). The ejecta velocity adopted here corresponds to a typical photospheric velocity (Wang et al. 2003) and might be lower than the terminal ejecta velocity (Wang 2006). However, the uncertainty resulting from the ejecta velocity is moderate and accepted. We will discuss its influence in Section 4. The rise time does not significantly affect the final results.

Meng et al. (2009) performed binary stellar evolution calculations for more than 25 000 close WD binary systems with various metallicities and Meng & Yang (2009) presented the distribution of all the parameters for these close systems before the RLOF and at the moment of the SN Ia explosion. Incorporating their results into the binary population synthesis code of Hurley et al. (2000, 2002), we obtain the distribution of the wind mass, M_{wind} (see Fig. 1) and the color excess via Equations (1) and (6). The basic parameters for Monte Carlo simulations are the same as those in Meng et al. (2009) when primordial binary samples are generated. Because the code is valid just for $Z \leq 0.03$, only five metallicities (i.e. $Z = 0.03, 0.02, 0.01, 0.004$ and 0.001) are examined here.

The greatest uncertainty of our model is from V_{wind} . Here, we assume that $V_{\text{wind}} = 10\text{ km s}^{-1}$ and we will discuss it in Section 4.

3 RESULTS

In Figure 2, we show the distribution of the color excesses of SNe Ia at maximum light for various metallicities. The distribution from observation is also shown by the solid histogram in the figure (Reindl et

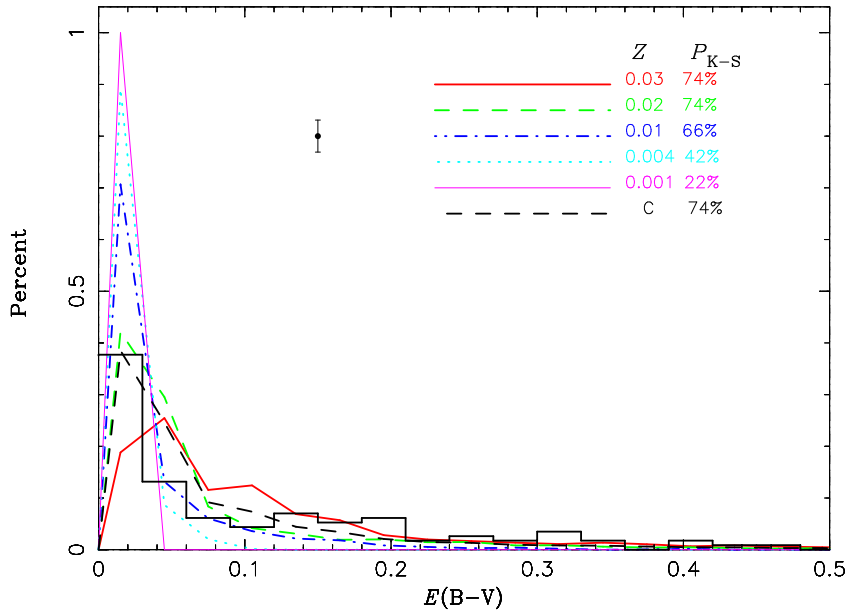


Fig. 2 Distribution of color excesses of SNe Ia at maximum light for various metallicities, where wind velocity is assumed to be 10 km s^{-1} . The solid histogram is from observation, and the bar represents its maximum error (Reindl et al. 2005). The black dashed line is the sum of those of $Z = 0.01, 0.02$ and 0.03 , where the weights for the three components are 20%, 40% and 40% respectively. Via K-S testing, the percentages indicated in the figure show the confidence level that the distributions of color excess from theory and observation are indistinguishable.

al. 2005). We see in the figure that the SD model with optically thick wind can reproduce the observed distribution of color excesses of SNe Ia. The K-S test shows that the cases of $Z = 0.02$ and $Z = 0.03$ have the highest confidence level that the distributions from theory and observation are indistinguishable. The sample of Reindl et al. (2005) includes the SNe Ia with various metallicities. However, it is difficult to determine the metallicity of the host galaxy of every SN Ia over a large distance (Hamuy et al. 2000). Wang et al. (2006) collected the properties of several SNe Ia from previous papers and noticed that the mean metallicity of the host galaxies of the SNe Ia is $[12 + \log(\text{O}/\text{H})]_{\text{mean}} = 8.85 \pm 0.10$ (private communication), which is consistent with solar metallicity $[12 + \log(\text{O}/\text{H})]_{\text{solar}} \sim 8.8$ (Zaritsky et al. 1994). Thus, our result is consistent with observation although the sample collected by Wang et al. (2006) is small.

There are some SNe Ia whose color excesses are very large (i.e. larger than 1.0), such as SN 1999cl (Jha 2002; Reindl et al. 2005), SN 2003cg (Elias-Rosa et al. 2006) and SN 2006X (Wang et al. 2008). In the sample of Reindl et al. (2005), only one of the 113 SNe Ia has a color excess larger than 1. In our simulation, the possibility of a high-color-excess SNe Ia is 2.0% for $Z = 0.03$, 0.4% for $Z = 0.02$ and 0 for $Z < 0.02$, consistent with observations. This result might imply that the SNe Ia may have a color excess larger than 1 only when their host galaxies have a metallicity larger than 0.02. Observationally, the host galaxies of SN 1999cl and SN 2006X, i.e. NGC 4501 and NGC 4321, are both oversolar galaxies (Caputo et al. 2000; Dors Jr & Copetti 2006). Although there is no information about the metallicity of the host galaxy of SN 2003cg (NGC 3169), NGC 3169 is an Sa galaxy and probably has an oversolar metallicity (Willner et al. 1985).

4 DISCUSSION

Our analytic model is very simple. We discuss various uncertainties in our model in this section.

4.1 Wind Velocity

The major uncertainty of our model is from the assumption that $V_{\text{wind}} = 10 \text{ km s}^{-1}$. Although the consistency between the theoretical distribution of color excess and that from observation upholds this assumption, there is no direct observational evidence to verify it. Many observational efforts were projected to find CSM (Hamuy et al. 2003; Aldering et al. 2006; Panagia et al. 2006; Ofek et al. 2007; Patat et al. 2007a,b), and only one observation obtained the constraint of the wind velocity (Patat et al. 2007a). The wind velocity is constrained to be smaller than 50 km s^{-1} (see fig. 2 in Patat et al. 2007a), and then Patat et al. suggested that the progenitor of SN 2006X should be a WD+RG system. However, we cannot rule out the possibility that the observed CSM is from the optically thick wind since the companion has not been directly observed (Hachisu et al. 2008). Recently, Badenes et al. (2007) explored the relationship between the SD models with optically thick wind for SNe Ia and the properties of the supernova remnants that evolve after the explosion. They found that an optically thick wind with a velocity larger than 200 km s^{-1} would excavate large low-density cavities around the progenitors. The large cavities are incompatible with the dynamics of the forward shock and the X-ray emission from the shocked ejecta in all the SNe Ia remnants that they examined. However, they also showed that if a wind velocity of 10 km s^{-1} is used, the properties of type Ia supernova remnants are very compatible with the prediction from the SD model with an optically thick wind. Generally, the escape velocity from a white dwarf is on the order of magnitude of 10^3 km s^{-1} , which is upheld by observations from recurrent novae (Wood & Lockley 2000). In the theoretical framework laid down by Hachisu et al. (1996), an optically thick wind is formed in a CO WD envelope with a photospheric velocity of $\sim 10^3 \text{ km s}^{-1}$ (Hachisu et al. 1999a,b), where the expansion of the photosphere is driven by helium flash in a helium shell on top of CO WD (Kato & Hachisu 1999). Thus, neither theory nor observation seem to uphold an assumption of a low wind velocity at present. We checked the influence of wind velocity on the distribution of color excess for the case of $Z = 0.02$ and the results are shown in Figure 3. We see in the figure that when $V \geq 100 \text{ km s}^{-1}$, K-S testing gives a low confidence level that the distributions of color excess

from theory and observation are indistinguishable, while when $V \leq 50 \text{ km s}^{-1}$, K-S testing shows an acceptable level. This result is similar to that in Badenes et al. (2007).

4.2 Delay Time

The secondary uncertainty of our model is from t_d . Since an optically thick wind may stop before an SN Ia explosion, t_d used in this paper overestimates the delay time of the wind for some systems. However, this is not a serious problem since for most cases, SNe Ia occur during the wind phase or after the wind phase for a short time (Han & Podsiadlowski 2004; Meng et al. 2009). In addition, t_d obtained from Equation (10) only approximates the mean value for a given M_2^i . This is also not a serious problem since we only check an average distribution of color excess. Generally, the peak of the distribution of color excesses moves to lower color excess with t_d , and the peak value increases while the percentage of high color excess SNe Ia decreases with t_d .

4.3 Metallicity

The combination of different metallicities is checked and shown in Figure 2 by the black dashed line since not all SNe Ia have the same metallicity. The weights of the components for $Z = 0.01, 0.02$ and 0.03 are simply fitted from the samples of Hamuy et al. (2000) and Wang et al. (2006). We also show the best fitted line in Figure 3 by the black dashed line. We can see from these lines that the combination of different metallicities does not significantly increase the confidence level that the distributions generated from theory and observation are indistinguishable. Actually, for any combination of $Z = 0.01, 0.02$ and 0.03 , the results will be acceptable, i.e. yielding a similar K-S test probability, which is derived from

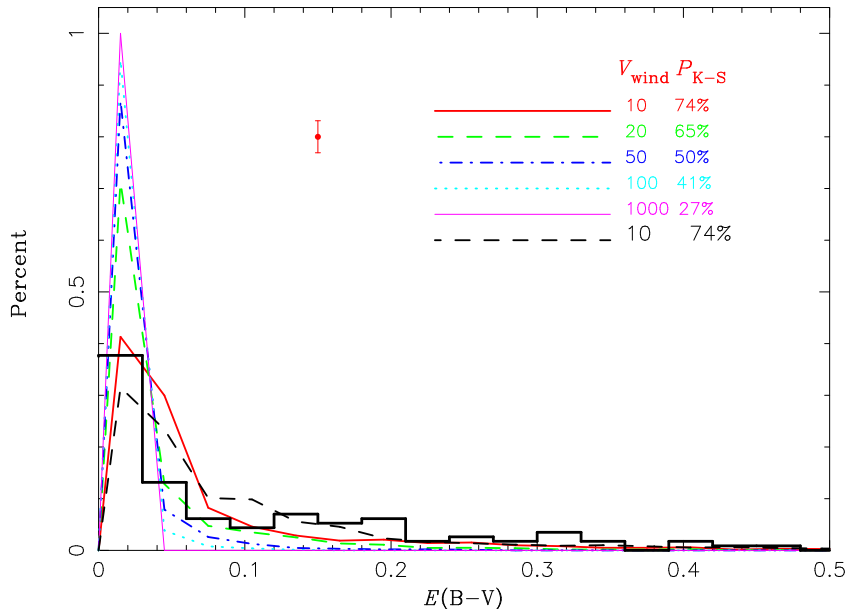


Fig. 3 Distribution of color excesses of SNe Ia at maximum light for $Z = 0.02$ and various wind velocities (in km s^{-1}). The solid histogram is from observation, and the bar represents its maximum error (Reindl et al. 2005). Via K-S testing, the percentages show the confidence level that the distributions of color excess from theory and observation are indistinguishable. The black dashed line is the best fitted line, where the weights for the components of $Z = 0.01, 0.02$ and 0.03 are 20%, 10% and 70%, respectively.

similar K-S test probabilities for the distributions of $Z = 0.01, 0.02$ and 0.03 . So, the basic results here still hold.

4.4 Interstellar Extinction

While we are not sure about the existence of the optically thick wind (it is a prediction by a model, not an observed fact, Hachisu et al. 1996), we are absolutely sure about the existence of the interstellar extinction (IE). In the paper, we did not consider the influence of IE since it is difficult to separate it from CSM dust. However, we know that Type Ia SNe, like other celestial objects, suffer from interstellar reddening, arising from material that has nothing to do with the circumstellar environment of the exploding star. Let us consider the case of SN 2006X, whose color excess is certainly larger than $E(B - V) = 1$, which most likely arises from a cold molecular cloud which has nothing to do with the explosion site (Wang et al. 2008). So, for the case of suffering interstellar reddening, we should remove the influence of IE on color excess. At present, it is very difficult to do this. However, it is a clear effect that IE will lead to certain directions to where parameters such as V_{Wind} and V_{ejec} should go, e.g. moving some very reddened observed SNe Ia to a lower reddened one would yield a higher V_{Wind} or V_{ejec} . For example, if we assume rather arbitrarily and simply that all observed SNe Ia suffer an extinction of $E(B - V)_{\text{host}} = 0.1$ within their host galaxies, our model suggests $V_{\text{Wind}} = 20 \text{ km s}^{-1}$ or $V_{\text{ejec}} = 20\,000 \text{ km s}^{-1}$. Similarly, if $E(B - V)_{\text{host}} = 0.2$, our model suggests $V_{\text{Wind}} = 50 \text{ km s}^{-1}$ or $V_{\text{ejec}} = 50\,000 \text{ km s}^{-1}$. So, the effect of IE could be counteracted by another uncertainty, V_{ejec} , and the basic results in this paper are still valid (see the discussion about ejecta velocity below).

If the color excess is from CSM, as shown in this paper, one may argue that we would have seen the CSM material through radio and X-ray emission, arising in the shock produced by the fast-moving SN ejecta crashing into the CSM (Stockdale et al. 2006). However, Panagia et al. (2006) showed a non-detection result in radio for 27 SNe Ia via the Very Large Array (VLA) observations, even including SN 2002ic, which indicated that the mass-loss rate should be lower than $\sim 3 \times 10^{-8} M_{\odot} \text{ yr}^{-1}$. We take a typical case to check whether our model contradicts the observations. We set the companion mass to $2.1 M_{\odot}$ (see fig. 10 in Meng et al. 2009), which corresponds to a delay time of $2.5 \times 10^6 \text{ yr}$. The mass of lost material is set to $0.3 M_{\odot}$ (see Fig. 1). The mean mass-loss rate is $12 \times 10^{-8} M_{\odot} \text{ yr}^{-1}$, which is higher but still comparable to that inferred from observations. Attempts to detect radio emission from SN 2002ic with the VLA were unsuccessful (Berger et al. 2003; Stockdale et al. 2003). SN 2002ic is the first case to show a CSM signal (Hamuy et al. 2003): the amount of CSM is $0.5\text{--}6 M_{\odot}$ (Wang et al. 2004; Chugai & Yungelson 2004; Uenishi et al. 2004; Kotak et al. 2004) and its properties may be explained successfully by the WD+MS model used here (Han & Podsiadlowski 2006). In addition, another recent twin of SN 2002ic (SN 2005gj, Aldering et al. 2006) has also not been detected using the VLA (Soderberg & Frail 2005). These non-detection results may indicate that the mechanism that is successfully used for SNe Ib/c may not work for SNe Ia (Panagia et al. 2006). So, our model is at least not inconsistent with observations at present.

4.5 Ionization and Ejecta Velocity

Generally, when an SN explodes, its radiation field is quite strong, especially at a distance $r_{\text{H}} < 10^{16} \text{ cm}$ (for SN 2006X, $r_{\text{H}} < 4 \times 10^{15} \text{ cm}$, Patat et al. 2007a). This radiation can easily ionize hydrogen and evaporate dust up to quite large distances, causing the disappearance of reddening. In our simple model, this effect is not considered completely. We will check the influence of the effect.

We set $r_{\text{H}} = 10^{16} \text{ cm}$ and assume that all hydrogen atoms are ionized within the shell with a radius of r_{H} . The column density of ionized hydrogen is $n_{\text{H},0} = \int_{r_1}^{r_{\text{H}}} ar^{-2} dr$, where $r_1 = 1.73 \times 10^{15} \text{ cm}$ (an ejecta velocity of 10^4 km s^{-1} and a rise time of 20 d are assumed). Then, the relative uncertainty from the ionization effect is $\frac{n_{\text{H},0}}{n_{\text{H}}} = \frac{(r_{\text{H},0} - r_1)r_{\text{m}}}{(r_{\text{m}} - r_1)r_{\text{H},0}} \simeq \frac{r_{\text{H},0} - r_1}{r_{\text{H},0}} \simeq 0.83$ ($r_{\text{m}} \gg r_1$). The uncertainty seems too large. However, this situation may be improved by taking a higher ejecta velocity and a smaller distance r_{H} . A distance of $r_{\text{H}} = 4 \times 10^{15} \text{ cm}$, like SN 2006X, may reduce the uncertainty to 0.57.

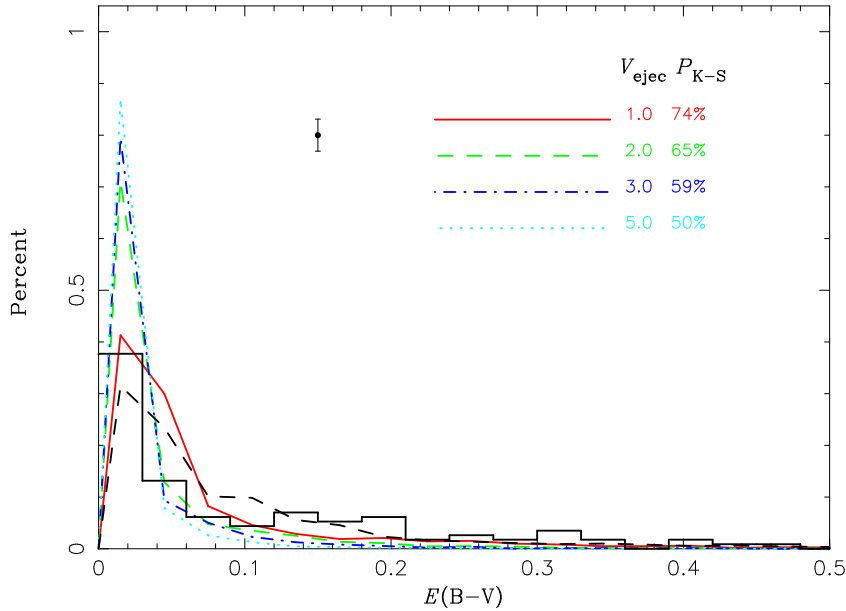


Fig. 4 Distribution of color excesses of SNe Ia at maximum light for different ejecta velocities, where wind velocity is assumed to be 10 km s^{-1} . The ejecta velocity is in units of 10^4 km s^{-1} . The black dashed line is the best fitted line, where the weights for the components of $Z = 0.01, 0.02$ and 0.03 are 20%, 10% and 70%, respectively.

The ejecta velocity used here may be smaller than the terminal velocity of SN Ia which can be as high as $3 \times 10^4 \text{ km s}^{-1}$ (Wang 2006). This value may reduce the uncertainty from the ionization effect to $0 \sim 0.48$, which means that no more than half of the CSM is evaporated up to large distances and has no influence on the color excess of SNe Ia. Then, the ionization effect at most decreases the confidence level that theory and observation are indistinguishable from 74% to 65%.

In Figure 4, we show the influence of ejecta velocity on the distribution of the color excess of SNe Ia. The influence is similar to that of wind velocity. From the figure, we can see that the peak of the distribution increases with the ejecta velocity, and when $V_{\text{ejec}} < 5 \times 10^4 \text{ km s}^{-1}$, the distributions of color excess from theory and observation are indistinguishable at a confidence level of higher than 50%. Fortunately, the effect of ionization and a higher ejecta velocity is the same as the interstellar effect, and their influences on the decrease of the confidence level may counteract each other. Thus, we can say that the distribution of color excess between theory and observation is indistinguishable at a level of higher than 59%, even when $V_{\text{ejec}} = 3 \times 10^4 \text{ km s}^{-1}$.

For the discussion above, our model may produce a meaningful result although our analytic model is rather simple.

5 SUMMARY AND CONCLUSIONS

In summary, if a wind velocity of $\sim 10 \text{ km s}^{-1}$ is adopted, the SD model with an optically thick wind may reproduce the distribution of color excess of SNe Ia obtained from observation, which might support the SD model for SNe Ia. However, if a wind velocity larger than 100 km s^{-1} is adopted, the reproduction is bad. Our results are similar to those of Badenes et al. (2007). Thus, the performance of more detailed observations about the velocity of CSM around progenitors of SNe Ia is encouraged.

Acknowledgements This work was funded by the National Natural Science Foundation of China (NSFC; Grant Nos.11080922 and 12345678).

References

- Aldering, G., Antilogus, P., Bailey, S., et al. 2006, *ApJ*, 650, 510
Badenes, C., Hughes, J. P., Bravo, E., et al. 2007, *ApJ*, 662, 472
Berger, E., Soderberg, A. M., & Frail, D. A. 2003, *IAUC*, 8157, 2
Bohlin, R. C., Savage, B. D., & Brake, J. F. 1978, *ApJ*, 224, 132
Branch, D., Fisher, A., & Nugent, P. 1993, *AJ*, 106, 2383
Branch, D. 2004, *Nature*, 431, 1044
Caputo, F., Marconi, M., Musella, I., et al. 2000, *MmSAL*, 71, 1041
Chen, W., & Li, X. 2007, *ApJ*, 658, L51
Chugai, N. N., & Yungelson, L. R. 2004, *Astronomy Letters*, 30, 65
Conley, A., Howell, D. A., Howes, A., et al. 2006, *AJ*, 132, 1707
Dors, Jr. O. L., & Copetti, M. V. F. 2006, *A&A*, 452, 473
Draine, B. T. 2003, *ARA&A*, 41, 241
Elias-Rosa, N., Benetti, S., Cappellaro, E., et al. 2006, *MNRAS*, 369, 1880
Fitzpatrick, E. L. 1985, *ApJ*, 299, 219
Gamezo, V. N., Khokhlov, A. M., Oran, E. S., et al. 2003, *Science*, 299, 77
Hachisu, I., Kato, M., & Nomoto, K. 1996, *ApJ*, 470, L97
Hachisu, I., Kato, M., Nomoto, K., & Umeda, H. 1999a, *ApJ*, 519, 314
Hachisu, I., Kato, M., & Nomoto, K. 1999b, *ApJ*, 522, 487
Hachisu, I., Kato, M., & Nomoto, K. 2008, *ApJ*, 679, 1390 (arXiv: 0710.0319)
Hamuy, M., et al. 2000, *AJ*, 120, 1479
Hamuy, M., et al. 2003, *Nature*, 424, 651
Han, Z., & Podsiadlowski, Ph. 2004, *MNRAS*, 350, 1301
Han, Z., & Podsiadlowski, Ph. 2006, *MNRAS*, 368, 1095
Han, Z. 2008, *ApJ*, 677, L109
Hillebrandt, W., & Niemeyer, J. C. 2000, *ARA&A*, 38, 191
Hurley, J. R., Pols, O. R., & Tout, C. A. 2000, *MNRAS*, 315, 543
Hurley, J. R., Tout, C. A., & Pols, O. R. 2002, *MNRAS*, 329, 897
Iben, I., & Tutukov, A. V. 1984, *ApJS*, 54, 335
Jha, S. 2002, Ph.D. thesis, Harvard Univ.
Kato, M., & Hachisu, I. 1999, *ApJ*, 513, L41
Koorneef, J. 1982, *A&A*, 107, 247
Kotak, R., Meikle, W. P. S., Adamson, S., et al. 2004, *MNRAS*, 354, L13
Langer, N., Deutschmann, A., Wellstein, S., et al. 2000, *A&A*, 362, 1046
Leibundgut, B. 2000, *A&ARv*, 10, 179
Li, X. D., & van den Heuvel, E. P. J. 1997, *A&A*, 322, L9
Lü, G., Zhu, C. Wang, Z., & Wang, N. 2009, *MNRAS*, 396, 1086, arXiv:0903.2636
Martin, N., Maurice, E., & Lequeux, J. 1989, *A&A*, 215, 219
Meng, X., Chen, X., & Han, Z. 2009, *MNRAS*, 395, 2103, arXiv:0802.2471
Meng, X., & Yang, W. 2009, *MNRAS*, arXiv: 0909.2167
Nomoto, K., Umeda, H., Hachisu, I., Kato, M., Kobayashi, C., & Tsujimoto, T. 1999, in *Type Ia Supernova: Theory and Cosmology*, eds. J. Truran, & T. Niemeyer (New York: Cambridge Univ. Press), 63
Nomoto, K., Uenishi, T., Kobayashi, C. Umeda, H., Ohkubo, T., Hachisu, I., & Kato, M. 2003, in *From Twilight to Highlight: The Physics of supernova*, ESO/Springer serious "ESO Astrophysics Symposia", eds. W. Hillebrandt, & B. Leibundgut (Berlin: Springer), 115
Ofek, E. O., Cameron, P. B., Kasliwal, M. M., et al. 2007, *ApJ*, 659, L13
Panagia, N., et al. 2006, *ApJ*, 646, 369
Patat, E., et al. 2007a, *Science*, 317, 924

- Patat, F., et al. 2007b, *A&A*, 474, 931, astro-ph/0708.3698
- Perlmutter, S., et al. 1999, *ApJ*, 517, 565
- Pols, O. R., Schröder, K. P., Hurly, J. R., et al. 1998, *MNRAS*, 298, 525
- Reindl, B., Tammann, G. A., Sandage, A., et al. 2005, *ApJ*, 624, 532
- Riess, A., et al. 1998, *AJ*, 116, 1009
- Soderberg, A. M., & Frail, D. A. 2005, *ATel*, 663, 1
- Stockdale, C. J., Sramek, R. A., Weiler, K. W., et al. 2003, *IAUC*, 8157, 3
- Stockdale, C. J., Maddox, L. A., Cowan, J. J., et al. 2006, *AJ*, 131, 889
- Strovink, M. 2007, *ApJ*, 671, 1084
- Uenishi, T., Suzuki, T., Nomoto, K., et al. 2004, *Rev. Mex. A&A*, 20, 219
- Wang, L., Baade, D., Höflich, P., et al. 2003, *ApJ*, 591, 1110
- Wang, L., Baade, D., Höflich, P., et al. 2004, *ApJ*, 604, L53
- Wang, L. 2005, *ApJ*, 635, L33
- Wang, L., Baade, D., Höflich, P., et al. 2006, *ApJ*, 653, 490
- Wang, X., Wang, L., Pain, R., et al. 2006, *ApJ*, 645, 488
- Wang, X., Li, W., Filippenko, A. V., et al. 2008, *ApJ*, 675, 626, arXiv:0708.0140
- Webbink, R. F. 1984, *ApJ*, 277, 355
- Whelan, J., & Iben, I. 1973, *ApJ*, 186, 1007
- Willner, S. P., Elvis, M., Fabbiano, G., et al. 1985, *ApJ*, 299, 443
- Wood, J. H., & Lockley, J. J. 2000, *MNRAS*, 313, 789
- Yungelson, L., Livio, M., Tutukou, A., & Kenyon, S. J. 1995, *ApJ*, 447, 656
- Zaritsky, D., Kennicutt, R. C. Jr., & Huchra, J. P. 1994, *ApJ*, 420, 87